Breaking Simple Scaling Relations Through Metal-Oxide Interactions: Understanding Room Temperature Activation of Methane on M-CeO_2 (M= Pt, Ni or Co) Interfaces

Pablo G. Lustemberg,[a,b],+ Feng Zhang,[c],+ Ramón A. Gutiérrez,[d] Pedro J. Ramírez,[d] Sanjaya D. Senanayake,*[e] José A. Rodriguez*[e] and M. Verónica Ganduglia-Pirovano*[b]

[a] Instituto de Fisica Rosario (IFIR), CONICET-UNR, Bv. 27 de Febrero 210bis, 2000EZP Rosario, Santa Fe, Argentina

[b] Instituto de Catálisis y Petroleoquímica, CSIC, C/Marie Curie 2, 28049 Madrid, Spain

[c] Department of Materials Science and Chemical Enginnering, SUNY at Stony Brook, Stony Brook, New York 11794, United States

[d] Facultad de Ciencias, Universidad Central de Venezuela, Caracas 1020-A, Venezuela

[e] Chemistry Division, Brookhaven National Laboratory, Upton, New York 11973, United States

ABSTRACT

The clean activation of methane at low temperatures remains an eminent challenge and a field of competitive research. In particular, on late transition metal surfaces such as Pt(111) or Ni(111), elevated temperatures are necessary to activate the hydrocarbon molecule, but a massive deposition of carbon makes the metal surface useless for catalytic activity. However, on very low-loaded M/CeO_2 (M= Pt, Ni, or Co) surfaces, the dissociation of methane occurs at room temperature, which is unexpected considering simple linear scaling relationships. This intriguing phenomenon has been studied using a combination of experimental techniques (ambient-pressure X-ray photoelectron spectroscopy, time-resolved X-ray diffraction and X-ray absorption spectroscopy) and density functional theory-based calculations. The experimental and theoretical studies show that the size and morphology of the supported nanoparticles together with strong metal-support interactions are behind the deviations from the scaling relations. These findings point toward a possible strategy to circumvent scaling relations, producing active and stable catalysts which can be employed for methane activation and conversion.

[+]P. G. Lustemberg and F. Zhang contributed equally to this work and should be regarded as co-first authors.

[*]Corresponding authors: M. Verónica Ganduglia-Pirovano (vgp@icp.csic.es); Sanjaya D. Senanayake (ssenanay@bnl.gov); José A. Rodriguez (rodrigez@bnl.gov)

TOC Graphic

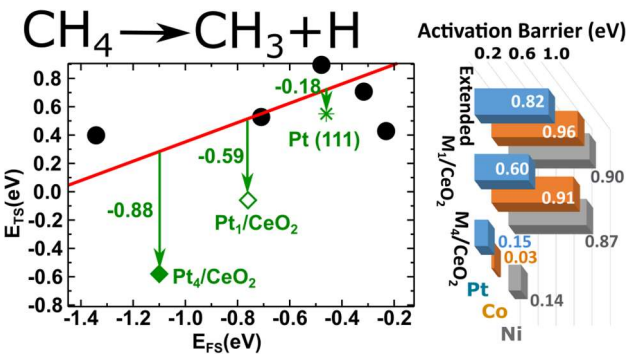
CH4 → CH3+H
-0.18
Pt (111)
-0.59
Pt1/CeO2
-0.88
Pt4/CeO2
ETS(eV)
EFS(eV)
Activation Barrier (eV)
0.2 0.6 1.0
Extended
M1/CeO2
M4/CeO2
0.82
0.96
0.60
0.90
0.91
0.15
0.87
0.03
0.14
Pt
Co
Ni

Methane (CH_4) is the simplest, most stable and abundant alkane molecule in our planet.[1] It is the main component of natural gas and a major problem in the atmosphere due to its contribution to greenhouse warming.[2-4] There is a broad interest in the activation and conversion of methane into value added chemicals (aromatics, olefins, oxygenates).[3, 4] This is a real challenge because of the high C–H bond strength (104 kcal/mol first bond dissociation energy), the absence of low-energy empty orbitals, and the presence of high energy occupied orbitals.[5, 6] When dealing with the activation of methane, several descriptors and scaling relations have been examined for the cleavage of the first C–H bond in the hydrocarbon.[5-11] In general, these descriptors and scaling relations provide guidelines to compare and predict the performance of potential new catalysts with that of existing materials used for C–H bond activation.[5, 6, 9] They can be used to quickly determine whether a new material of interest can successfully activate methane and should be examined further.[5, 6, 9] Computational volcanos have become the gold standard in the design of catalysts and scaling relations are generally considered to have a universal validity.[6, 10, 12] In this work, we investigate how to use metal-support interactions to break simple scaling relations and enhance catalytic activity for methane activation.

The probability of methane dissociation on the surface of late transition metals is rather low.[13-15] The (111) surface of these metals is typically used as a benchmark in studies of C–H bond activation.[16-18] For example, on the clean Pt(111) surface, the methane C–H dissociation probability is close to 1×10^{-8} at 25 °C.[15] At room temperature, the dissociation results in deposited C and CH_x species on the platinum surface, and upon heating to 100–200 °C, the amount of adsorbed C increases and C–C coupling occurs generating ethylidyne (C_2H_3) and ethynyl (C_2H) species.[15] A carbonaceous layer eventually inhibits further dissociation of the C–H bond on Pt(111), deactivating its chemical and catalytic properties.[15] Pt(100) and Pt(110)-(1×2) are more reactive towards methane than Pt(111),[17, 18] but they still have problems with

C–H bond breaking and undergo deactivation by the formation of a carbonaceous layer. Ni(111) and many surfaces of other late transition metals are also not efficient for the activation of methane.[13, 16] A few oxide (IrO_2) and low-loaded metal/oxide (M/CeO_2, M= Ni or Co) systems can activate methane at low temperature.[19-22] On the latter, it has been found that cooperative interactions between a single cation and an oxide centre can lead to a cleavage of the first C–H bond in methane with an effective energy barriers that are below 0.7 eV.[19-23] But how general is this observation? It is important to establish if this type of phenomenon also occurs for other metal/oxide systems such as the Pt/CeO_2 surface, since recent studies point to special electronic and chemical properties for Pt atoms in contact with ceria,[24-26] but no systematic study has been performed for the interaction of methane with Pt/CeO_2.

In this work, we use a combination of experimental techniques (ambient-pressure X-ray photoelectron spectroscopy, time-resolved X-ray diffraction and X-ray absorption spectroscopy) and density functional theory-based calculations to study in detail the binding and activation of methane on Pt/CeO_2 surfaces with different configurations. After comparing with previous studies reported for Ni/CeO_2 and Co/CeO_2,[20, 21] our results reveal that the existence of Metal ↔ CeO_2 interactions result in significant deviations from simple scaling relations for the prediction of the activation energy barrier for the cleavage of the first C–H bond in CH_4,[6, 10] which are particularly large for low-loaded Pt/CeO_2 systems, producing active and stable catalysts for methane activation at room temperature conditions.

The reaction of methane with a $Pt/CeO_2(111)$ surface and a Pt/CeO_2 powder at temperatures between 25 and 427 ºC was investigated using ambient-pressure X-ray photoelectron spectroscopy (AP-XPS). [For details on the preparation of the Pt-CeO_2 interfaces, see Supporting Information.][21] The top panel in Figure 1 shows C 1s X-ray photoelectron spectra collected after exposing plain $CeO_2(111)$ and a surface pre-covered with 0.15 ML of platinum to 1 Torr of CH_4 at 25 °C. Neither $CeO_2(111)$ nor a ceria powder sample

were able to dissociate the hydrocarbon molecule at 25 °C. However, we did observe dissociation of methane upon interaction with the low-loaded (Θ_{Metal}= 0.15 ML) Pt/CeO_2(111) system. A peak around 284.8 eV points to the presence of CH_x (x= 1,2,3) fragments on the surface, produced by the partial dissociation of methane ($CH_4 \rightarrow CH_x + (4 - x)$ H).[20-22] A second peak around 290 eV indicates the formation of CO_x species as a consequence of the full dissociation of methane.[20-22] When compared to other low-loaded M/CeO_2(111) (M= Cu, Ni or Co) systems,[20-22] Pt/CeO_2(111) produces the largest amount of CH_x and the lowest amount of CO_x. This is very important if one is interested in the subsequent transformation of the CH_x fragments.

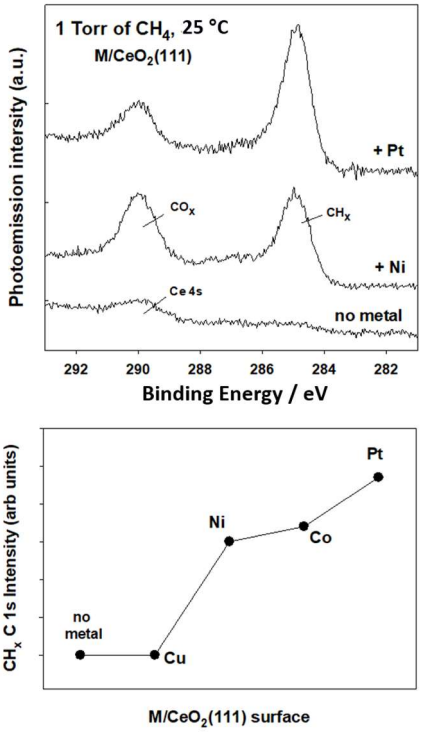

Figure 1. Top panel: C 1s X-ray photoelectron spectra recorded after exposing Pt/CeO_2(111) and CeO_2(111) to 1 Torr of methane at 25 °C. For comparison, the corresponding spectrum for a Ni/CeO_2(111) surface is also included. The coverage of Pt and Ni on ceria is ~ 0.15 ML. Bottom panel: Amount of CH_x species formed on M/CeO_2(111) surfaces. The results for Ni, Cu and Co were extracted from refs. 20, 21.

Furthermore, we found that the CH_x species were not too strongly bound to the Pt/CeO_2(111) surface. When the CH_x/Pt/CeO_2(111) surface was heated to 150 °C, the CH_x completely desorbed from the surface (as a mixture of CH_4, C_2H_6 and C_2H_4) and we did not see

the generation of a poisonous carbonaceous layer as reported for Pt(111).[15] Thus, the electronic perturbations induced by CeO_2(111) on Pt[24] allow the efficient dissociation of methane and prevent the formation of ethylidyne and ethynyl.

Figure 2 shows Pt 4f ambient-pressure photoelectron spectra for model Pt/CeO_2(111) and powder 0.5 wt% Pt/CeO_2 catalytic systems, upon their interaction with CH_4. The Pt $4f_{7/2}$ peaks at 72.7 and 73.3 eV in Pt/CeO_2(111) and 0.5 wt% Pt/CeO_2, respectively indicates that $Pt^{\delta+}$ species are dominant on the as-prepared sample surfaces. Initially, these systems have a mixture of 2+, 1+ and 0 oxidation states for platinum, and the proportion of these states changes when going from the model to the powder system (see Figure S1 and Table S1 for the fitting result). For the initial systems, Pt^{1+} was the dominant feature in Pt/CeO_2(111), whereas Pt^{2+} was present in the Pt/CeO_2 powder. Upon interaction with methane at 25 °C, the Pt 4f peaks got broader and the peak valley became shallower for both Pt/CeO_2(111) and 0.5 wt% Pt/CeO_2 systems. A shoulder peak also appeared at 77.2 eV on the model system and at 77.7 eV on the powder catalyst, and this can be attributed to the adsorption of carbon-containing species on Pt as a result of methane dissociation.

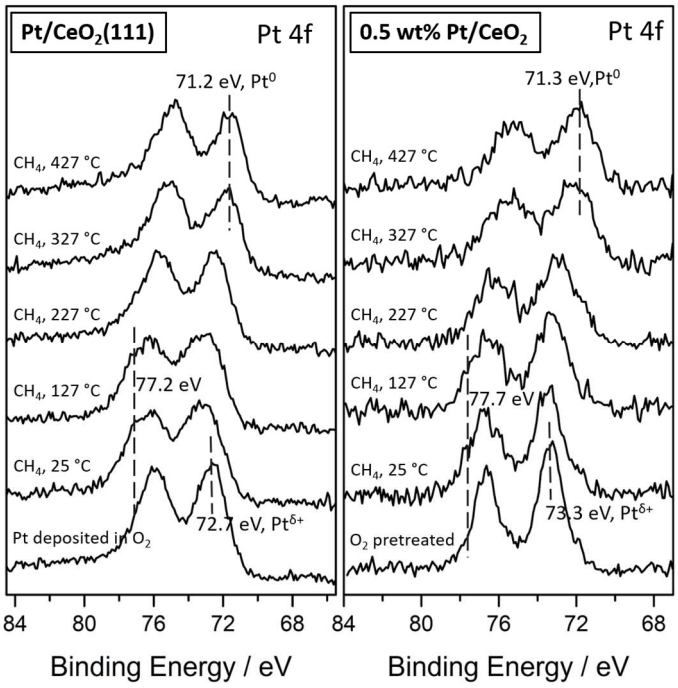

Figure 2. Pt 4f AP-XPS of $Pt/CeO_2(111)$ (left) and 0.5 wt% Pt/CeO_2 (right) under a methane atmosphere at low and elevated temperatures. The powder catalyst was pre-treated in 10 mTorr O_2 at 400 °C to remove any surface-bounded carbon species, and the samples were exposed to a 50 mTorr CH_4 during the reaction process.

As the temperature increases from 25 ºC to 427 ºC, the $Pt^{\delta+} \rightarrow Pt^0$ transformation occurs,[27, 28] which was already complete at 327 °C. A $Pt^{\delta+} \rightarrow Pt^0$ reduction at > 300 °C was also seen in experiments of in-situ X-ray absorption spectroscopy (XAS) for the Pt/CeO_2 powder sample. At these elevated temperatures, ceria reduction by methane was observed in the corresponding spectra of Ce 3d AP-XPS (Figure S2). In the case of the Pt/CeO_2 powder, this was also detected in results of time-resolved XRD where an expansion of the ceria lattice was found as a consequence of the formation of Ce^{3+} (Figure S3). In summary, at room temperature, small platinum particles in contact with ceria, which contain $Pt^{\delta+}$ species, are able to dissociate the methane molecule, producing mainly adsorbed CH_x fragments with a small amount of CO_x groups. At elevated temperatures, more than a monolayer of methane reacted with the systems producing Pt^0 and CeO_{2-x}. The reduction of the ceria is quite important because the oxide and supported metal could now cooperate in the catalytic conversion of methane to high value chemicals.

On the stoichiometric $CeO_2(111)$ surface, Pt adatoms on a bridge site, coordinated to two oxygen and one cerium atoms (Figure 3a), transfer the 6s electron to the empty 4f band of ceria, generating one Ce^{3+} ion, and thus are oxidized to Pt^{1+}, in agreement with previous results,[27, 29] (for details on the models and computational methods, see the Supporting Information). A planar rhombohedral Pt_4 cluster on $CeO_2(111)$ also reduces the ceria support with the formation of two Ce^{3+} (Figure 3a), and thus the average oxidation state of the Pt atoms is +0.5. The theoretical $Pt/CeO_2(111)$ model systems mimic the essential features of the experimental catalysts at room temperature ($Pt^{\delta+}/CeO_2$) (Figure 2). In short, as a result of strong metal-support interactions, Pt atoms in direct contact with the stoichiometric CeO_2 support

become oxidized to $Pt^{\delta+}$. On the reduced CeO_{2-x} support, modelled using the $Ce_2O_3(0001)$ surface (Figures S4 and S5), the interfacial Pt atoms recover their metallic character ($Pt^{\delta+} \rightarrow Pt^0$).

The dissociation of CH_4, i.e., $CH_4 \rightarrow CH_3$+H, on the extended Pt(111) surface is very difficult at room temperature due to a large energy barrier of 0.82 eV (Figure 3b and S5), in line with previous works.[18, 30, 31] In contrast, the dissociation probability of methane at room temperature on Pt atoms and small (flat) Pt_4 nanoparticles on CeO_2, with all the Pt atoms being interfacial and thus cationic, is expected to be significant since the energy barriers are $\lessapprox$ 0.6 eV (Figure 3b,c), in agreement with the experiments shown in Figure 1. This conclusion is further supported by the calculated Gibbs free energy profiles at 300 K and 1 atm CH_4 (Figure 3b), which indicate that there is essentially no effective free energy barrier (i.e., with respect to CH_4 in the gas phase) for the activation of methane on CeO_2-supported Pt atoms and small Pt_4 nanoparticles at normal conditions.

For surface-stabilized methane activation pathways, Latimer et al.[6] have proposed the existence of a linear scaling relation between the energy of the transition state structure for methane activation, E_{TS} (referenced to gas-phase CH_4 and the clean surface), and that of the final state, $E_{FS}=E_{CH_3+H}$, according to which stronger CH_3+H binding energies correspond to lower E_{TS} energies, as shown in Figure 4. It has been concluded that the model can accurately describe a wide range of materials such as CaO, MgO, PdO, doped MoS_2, rutile oxides in addition to clean as well O- and OH-promoted metals (black dots in Figure 4). To determine the applicability of this model to catalysts consisting of low-loaded metal clusters on ceria surfaces, the points corresponding to the E_{TS} and E_{FS} values for the cleavage of the first C–H bond in CH_4 on M_1 atoms and M_4 clusters (M= Pt, Co, Ni) on the $CeO_2(111)$ surface, as well as on the extended Pt(111), Co(0001) and Ni(111) surfaces (Table S2), have been added to Figure 4. For the purpose of comparison, the non-ZPE-corrected energy values have been used.

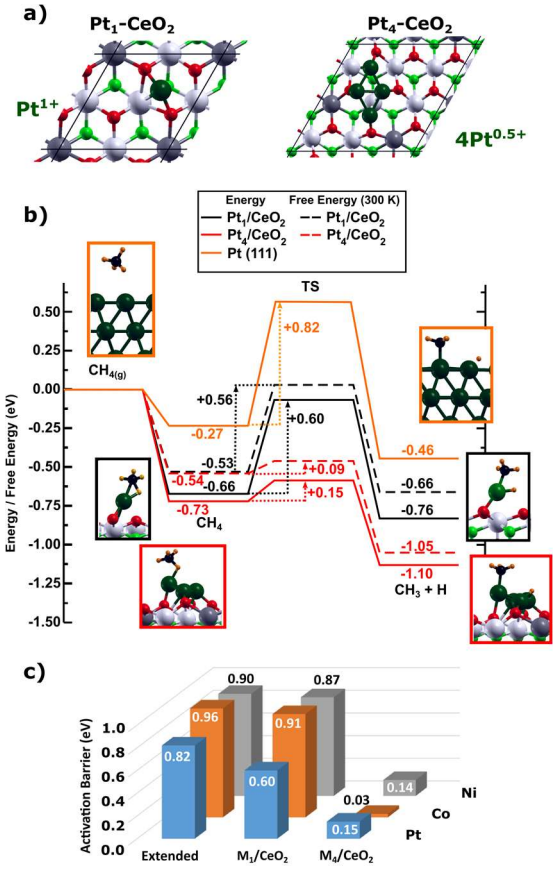

Figure 3. a) Atomic structure of Pt_1/ and $Pt_4/CeO_2(111)$. b) Energy (non-ZPE-corrected, solid lines) and Gibbs free energy profiles at 300 K, 1 atm of CH_4 (dashed lines) for the $CH_4 \rightarrow CH_3$+H reaction on Pt atoms and Pt_4 clusters on $CeO_2(111)$. The structures shown on the left and right of the reaction pathways correspond to the side views of the optimized initial (molecularly adsorbed) and final (dissociated) states used in the search of the transition state structure (TS). c) Activation energy barriers (non-ZPE-corrected) for M_1/ and $M_4/CeO_2(111)$ (M= Pt, Co, Ni) and for the extended M(111) (M= Pt, Ni) and Co(1000) surfaces.

The calculated E_{TS} values for the extended metal surfaces do not deviate much (up to ~0.20 eV, Figure 4, Table S3) from those predicted by the linear scaling relation, as it has already been observed by Latimer et al.[6] However, substantial deviations, ΔE_{TS}, from the predicted E_{TS} values are generally observed for the ceria-supported metal clusters. For example, for the most active system for C–H activation at room temperature, *i.e.*, Pt/CeO_2, the computed E_{TS} values are such that the C–H activation barriers over interfacial $Pt^{\delta+}$ sites on low-loaded Pt/CeO_2 surfaces are by up to ~0.9 eV *smaller* than the ones predicted by the linear scaling

relation. Understanding the origin of these deviations may provide crucial knowledge on how to circumvent the limitations on the activity of metal-based catalysts for methane activation.

On the Pt/CeO_2 surfaces, the $CH_4 \rightarrow CH_3$+H reaction is generally more exothermic than on Pt(111) (cf. Table S2, S4 and Figure S7). (In the following discussion, for the sake of clarity, we use non-ZPE-corrected energy values.) For example, for Pt_4/CeO_2, the reaction energy is –0.37 eV, whereas for Pt(111) is –0.19 eV (Figure 3a). We note that the small supported clusters feature a high degree of lability since they easily deform upon interaction with CH_4 and CH_3+H (cf. Figures S8, S9), in line with recently reported results for low-loaded Ni/TiC surfaces.[32] Moreover, the first important thing to note is that the CH_3+H fragments bind substantially stronger on the Pt/CeO_2 surfaces than on Pt(111), with the calculated final state energy, E_{FS}, following the Pt_4/CeO_2 (–1.10 eV) > Pt_1/CeO_2 (–0.76 eV) >> Pt(111) (–0.46 eV) trend (Figures 3, 4, and Table S3). According to the positive linear scaling relation between E_{FS} and E_{TS},[6] the *predicted* transition state energies are +0.30, +0.53, and +0.73 eV for the Pt_4/CeO_2, Pt_1/CeO_2 and Pt(111) surfaces, respectively, see Figure 4 and Table S3. That is, lower transition state energies by up to about 0.4 eV are already predicted for the CH_4 to CH_3+H reaction over $Pt^{\delta+}$ sites of the Pt/CeO_2 systems as compared to Pt(111). However, the here *calculated* transition states of the Pt/CeO_2 catalysed reaction are much *more stable* than those predicted by the linear scaling relationship (Figure 4), with deviations in the E_{TS} values of ΔE_{TS} = –0.88, –0.59, and –0.18 eV for the Pt_4/CeO_2, Pt_1/CeO_2 and Pt(111) surfaces, respectively (cf. –0.58, –0.06, and +0.55 eV for the actual E_{TS} calculated for Pt_4/CeO_2, Pt_1/CeO_2 and Pt(111), respectively, in Table S3).

With regard to the differences between the predicted *vs.* calculated activation energy barriers, $E_{Barrier}$, between the initial (molecularly chemisorbed) state, E_{IS}, and the transition state, E_{TS}, exactly the same differences as found between the predicted *vs.* calculated energies of the transition states exist (*i.e.*, $\Delta E_{Barrier} = \Delta E_{TS}$, Table S3). For the Pt/CeO_2 surfaces, the

predicted activation energies do not differ much from that for Pt(111), cf., 1.03, 1.19, and 1.00 eV for the Pt_4/CeO_2, Pt_1/CeO_2 and Pt(111) surfaces, respectively (Table S3). However, the corresponding calculated barriers, i.e., 0.82, 0.6, and 0.15 eV, do differ, and much, which is consistent with the observed more facile dissociation of the first C–H bond over Pt/ceria as compared to Pt(111), as already mentioned (Figure 3b, c). This is precisely due to the fact that the magnitude of the deviations $\Delta E_{Barrier}$ is system dependent, following the Pt(111) (0.18 eV) << Pt_1/CeO_2 (0.59. eV) < Pt_4/CeO_2 (0.88 eV) trend.

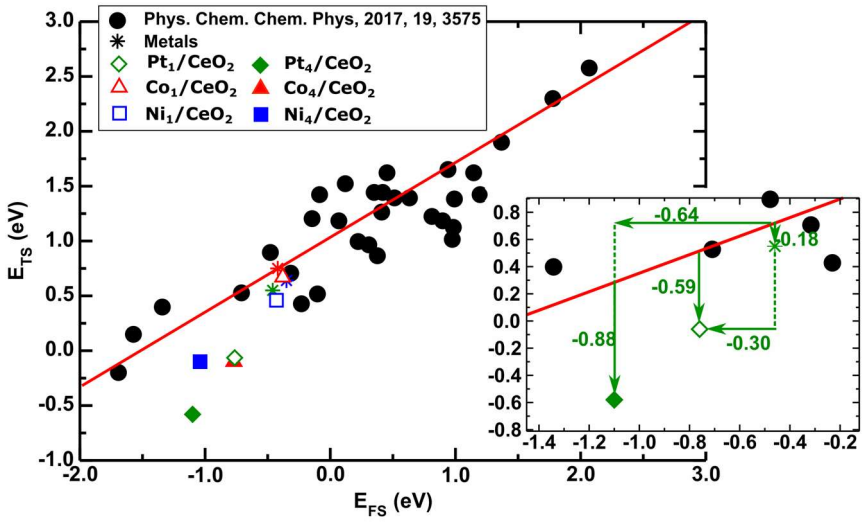

Figure 4. Scaling relation for the surface-stabilized pathway (E_{TS}=0.67 E_{FS}+ 1.04), according to ref. 6. Included are the (non-ZPE-corrected) E_{TS} and E_{FS} values for M_1 atoms and M_4 clusters (M= Pt, Co, Ni) on the CeO_2(111), as well as on the extended Pt(111), Co(0001) and Ni(111) surfaces.

The factors leading to the larger deviations from the linear scaling between E_{FS} and E_{TS} for the Pt/CeO_2 systems, as compared to the extended Pt(111) surface, are also related to the distinct adsorption properties of the former. With this regard, the second important thing to note is that not only the CH_3+H fragments bind stronger on the Pt/CeO_2 surfaces than on Pt(111), but also the CH_4 molecule. The DFT calculations reveal that the interaction between methane and the electronically modified $Pt^{\delta+}$ atoms in direct contact with the CeO_2 support, with adsorption energies of about –0.7 eV, is much stronger than that with the Pt(111) surface, with

a binding of about −0.3 eV (Figure 3b). The enhancement of the CH_4 adsorption energy on the low-loaded Pt/CeO_2 systems favours the probability of the reaction. The careful inspection of the interaction between CH_4 and the systems' surfaces reveal that the CH_4 molecules on Pt/CeO_2 come closer to the surface than on Pt(111), cf. the C–Pt distance of 2.20 and 2.34 Å for Pt_1 and Pt_4/CeO_2, respectively, with 3.52 Å for Pt(111) (Figures S8, S9, and S12), and thus charge transfer is enhanced at the interface. In both the Pt_1 and Pt_4/CeO_2 systems, the direction of the charge transfer is to the adsorbate, as reflected by the increase in the Bader charge for the C atom upon CH_4 adsorption, namely, 0.14 and 0.16*e* for Pt_1 and Pt_4/CeO_2, respectively, with respect to the gas-phase molecule (Table S5). Moreover, the final important thing to note is that on the Pt/CeO_2 surfaces, the C–H bond that will ultimately be cleaved, appears to be activated with a substantially elongated bond distance (1.26 and 1.19 Å for Pt_1 and Pt_4/CeO_2, respectively, Figure S8 and S9), whereas the variation in the other three C–H bonds is almost negligible, which is behind the facile dissociation of the first C–H bond on the low-loaded Pt/CeO_2 systems. A similarly strong CH_4 adsorption has been recently reported on $Pt_1/TiO_2(110)$.[9] Also, the higher CH_4 binding on a two-layer-thick PdO(101) film on Pd(100) as compared to a one-layer film,[33] which is accompanied by a significant reduction of the activation barrier for CH_4 dissociation on the former, has been discussed in terms of a ligand effect as a consequence of the presence of an oxygen atom directly below the Pd atom over which CH_4 dissociates in the thicker PdO film. Such an effect is also present in the Pt/CeO_2 systems (see Figure S6 and accompanying text in the Supporting Information).

Figure 3c compares the activation energy barrier for the CH_4 to CH_3+H reaction on $CeO_2(111)$-supported M_1 atoms and M_4 clusters (M= Pt, Co, Ni) as well as on the Pt(111), Co(0001) and Ni(111) extended metal surfaces. In comparison with ceria-supported single Pt atoms and small Pt_4 clusters, the anchoring of Co and Ni atoms on the stoichiometric $CeO_2(111)$ surface yields Co^{2+} and Ni^{2+} species and two Ce^{3+} ions,[20-22] respectively (Figure S4). In the

planar Co_4 and Ni_4 on $CeO_2(111)$, the average oxidation state of the Co and Ni atoms are +0.75 and +0.5, respectively (Figure S5). It is clear that in all cases, the combined effect of the low metal loading and the ceria support results in the lowering of the activation barrier (Figure 3c). However, the amounts by which the linear scaling relation is "broken", are larger for the Pt_1 and Pt_4/CeO_2 systems, as compared to the corresponding Co/CeO_2 and Ni/CeO_2 ones (Figure 4 and Table S3). The comparison of the molecular binding, the activation and the dissociative adsorption of CH_4 on $CeO_2(111)$-supported M_1 atoms and M_4 clusters (M= Pt, Co, Ni) reveals that the use of Pt is able to strongly enhance the adsorption of methane molecules (cf. the calculated E_{IS} values in Table S3) and that from the resulting initial structures, the cleavage of the first C–H bond is easier, as compared to the Co/CeO_2 and Ni/CeO_2 systems (Figures S8 and S9). It is important to note that the activation energy barriers for the recombination reaction, $CH_3+H \rightarrow CH_4$, are also lower when Pt is used (cf., e.g., 0.52, 0.65, 0.94, and 1.01 eV for the Pt_4/CeO_2, Co_4/CeO_2, Co_4/CeO_2 and Pt(111) surfaces), which is in line with the finding that upon heating (150 ^oC), the CH_x desorbed from the Pt/CeO_2 surface without detecting the formation of carbonaceous species, as it was the case for Pt(111).[15]

We finally mention that in line with a stronger binding of the CH_3+H final state on $Ce_2O_3(0001)$-supported metallic M_1 atoms and M_4 clusters (M= Pt, Co, Ni) than on the corresponding extended metal surfaces, the CH_4 activation energy barriers are smaller for the low-loaded M^0/Ce_2O_3 systems, but the deviations of the calculated values from those predicted by the linear scaling relation, $\Delta E_{Barrier}$, lie within an energy range of about 1 eV (see Supporting Information). This is because on the small ceria-supported metal clusters, the CH_4 binding can be enhanced compared to that on the extended metal surfaces.

Our results for a range of low-loaded metal-ceria systems, including extended metal surfaces for comparison, show that the proposed linear scaling relation to predict the energy barrier for the activation of methane, does *not* generally hold for ceria-supported metal

nanoparticles. Strong interactions between the small metal particles in direct contact the with the ceria support lead to the stabilization of both the CH_4 molecule and the CH_3+H dissociation product, producing active and stable catalysts for methane activation under very mild conditions. The very low-loaded Pt/CeO_2 system is the best in terms of activity for methane dissociation and stability. The results illustrate how one can manipulate metal-support interactions to improve catalytic activity and stability, a major goal in heterogeneous catalysis.

ACKNOWLEDGEMENTS

The research carried out at the Brookhaven National Laboratory (BNL) was supported by the U.S. Department of Energy, Office of Science and Office of Basic Energy Sciences under contract No. DE-SC0012704. The XRD experiments carried out at the Advanced Photon Source Beamline 17BM (XRD) at Argonne National Laboratory were supported by the U.S. DOE under Contract No. DE-AC02-06CH11357. This project also received funding from the European Union's Horizon 2020 research and innovation programme under the Marie Skłodowska-Curie grant agreement No 832121. Computer time provided by the BIFI-ZCAM, the RES (Red Española de Supercomputación) resources at MareNostrum 4 (BSC, Barcelona) and Altamira (IFCA, Cantabria) nodes, the Piluso node within SNCAD (Sistema Nacional de Computación de Alto Desempeño, Argentina), is acknowledged. Computer time provided by the DECI resources at Finis Terrae II based in Spain at CESGA, with the support from PRACE aislb, is also acknowledged. M.V.G.P. thanks the support by the MINECO and MICINN-Spain (CTQ2015-71823-R and RTI2018-101604-B-I00, respectively).

Data availability

The data that support the plots within this paper and other findings of this study are available from the corresponding authors on reasonable request. The DFT data are available from the NOMAD Repository https://repository.nomad-coe.eu/ with the identifier doi: 10.17172/NOMAD/2020.02.18-3.

References

1. Feichter, J.; Schurath, U.; Zellner, R., Luftchemie und Klima. *Chemie in unserer Zeit* **2007,** *41* (3), 138-150.
2. Thornton, P. K., Livestock production: recent trends, future prospects. *Philosophical transactions of the Royal Society of London. Series B, Biological sciences* **2010,** *365* (1554), 2853-2867.
3. Tang, P.; Zhu, Q.; Wu, Z.; Ma, D., Methane Activation: The Past and Future. *Energy Environ. Sci.* **2014,** *7* (8), 2580-2591.
4. Bousquet, P.; Ciais, P.; Miller, J. B.; Dlugokencky, E. J.; Hauglustaine, D. A.; Prigent, C.; Van der Werf, G. R.; Peylin, P.; Brunke, E. G.; Carouge, C.; Langenfelds, R. L.; Lathière, J.; Papa, F.; Ramonet, M.; Schmidt, M.; Steele, L. P.; Tyler, S. C.; White, J., Contribution of Anthropogenic and Natural Sources to Atmospheric Methane Variability. *Nature* **2006,** *443* (7110), 439-443.
5. Aljama, H.; Nørskov, J. K.; Abild-Pedersen, F., Tuning Methane Activation Chemistry on Alkaline Earth Metal Oxides by Doping. *J. Phys. Chem. C* **2018,** *122* (39), 22544-22548.
6. Latimer, A. A.; Aljama, H.; Kakekhani, A.; Yoo, J. S.; Kulkarni, A.; Tsai, C.; Garcia-Melchor, M.; Abild-Pedersen, F.; Norskov, J. K., Mechanistic Insights into Heterogeneous Methane Activation. *Phys. Chem. Chem. Phys.* **2017,** *19* (5), 3575-3581.
7. Weaver, J. F.; Hakanoglu, C.; Antony, A.; Asthagiri, A., Alkane activation on crystalline metal oxide surfaces. *Chem. Soc. Rev.* **2014,** *43* (22), 7536-7547.
8. Tsuji, Y.; Yoshizawa, K., Adsorption and Activation of Methane on the (110) Surface of Rutile-type Metal Dioxides. *J. Phys. Chem. C* **2018,** *122* (27), 15359-15381.
9. Fung, V.; Tao, F.; Jiang, D.-e., Low-temperature activation of methane on doped single atoms: descriptor and prediction. *Phys. Chem. Chem. Phys.* **2018,** *20* (35), 22909-22914.
10. Latimer, A. A.; Kulkarni, A. R.; Aljama, H.; Montoya, J. H.; Yoo, J. S.; Tsai, C.; Abild-Pedersen, F.; Studt, F.; Nørskov, J. K., Understanding trends in C–H bond activation in heterogeneous catalysis. *Nat. Mater.* **2017,** *16* (2), 225-229.
11. Ma, X.; Sun, K.; Liu, J.-X.; Li, W.-X.; Cai, X.; Su, H.-Y., Single Ru Sites-Embedded Rutile TiO2 Catalyst for Non-Oxidative Direct Conversion of Methane: A First-Principles Study. *J. Phys. Chem. C* **2019,** *123* (23), 14391-14397.
12. Pérez-Ramírez, J.; López, N., Strategies to break linear scaling relationships. *Nat. Catal.* **2019,** *2* (11), 971-976.
13. Choudhary, T. V.; Aksoylu, E.; Wayne Goodman, D. J. C. r., Nonoxidative activation of methane. *Catal. Rev.* **2003,** *45* (1), 151-203.
14. Schoofs, G. R.; Arumainayagam, C. R.; McMaster, M. C.; Madix, R. J., Dissociative chemisorption of methane on Pt(111). *Surf. Sci.* **1989,** *215* (1), 1-28.
15. Marsh, A. L.; Becraft, K. A.; Somorjai, G. A. J. T. J. o. P. C. B., Methane dissociative adsorption on the Pt (111) surface over the 300− 500 K temperature and 1− 10 Torr pressure ranges. *J. Phys. Chem. B* **2005,** *109* (28), 13619-13622.
16. Weaver, J., The adsorption and reaction of low molecular weight alkanes on metallic single crystal surfaces. *Surface Science Reports* **2003,** *50* (4-5), 107-199.
17. Petersen, M. A.; Jenkins, S. J.; King, D. A., Theory of Methane Dehydrogenation on Pt{110}(1 × 2). Part I: Chemisorption of CHx (x = 0 −3). *The Journal of Physical Chemistry B* **2004,** *108* (19), 5909-5919.
18. Nave, S.; Tiwari, A. K.; Jackson, B., Methane dissociation and adsorption on Ni(111), Pt(111), Ni(100), Pt(100), and Pt(110)-(1×2): Energetic study. *The Journal of Chemical Physics* **2010,** *132* (5), 054705.

19. Liang, Z.; Li, T.; Kim, M.; Asthagiri, A.; Weaver, J. F. J. S., Low-temperature activation of methane on the IrO2 (110) surface. *Science* **2017,** *356* (6335), 299-303.
20. Lustemberg, P. G.; Ramírez, P. J.; Liu, Z.; Gutierrez, R. A.; Grinter, D. G.; Carrasco, J.; Senanayake, S. D.; Rodriguez, J. A.; Ganduglia-Pirovano, M. V. J. A. C., Room-temperature activation of methane and dry re-forming with CO2 on Ni-CeO2 (111) surfaces: Effect of Ce3+ sites and metal–support interactions on C–H bond cleavage. *ACS Catal.* **2016,** *6* (12), 8184-8191.
21. Liu, Z.; Lustemberg, P.; Gutiérrez, R. A.; Carey, J. J.; Palomino, R. M.; Vorokhta, M.; Grinter, D. C.; Ramírez, P. J.; Matolín, V.; Nolan, M.; Ganduglia-Pirovano, M. V.; Senanayake, S. D.; Rodriguez, J. A., In Situ Investigation of Methane Dry Reforming on Metal/Ceria(111) Surfaces: Metal–Support Interactions and C–H Bond Activation at Low Temperature. *Angew. Chem. Int. Ed.* **2017,** *56* (42), 13041-13046.
22. Liu, Z.; Grinter, D. C.; Lustemberg, P. G.; Nguyen-Phan, T. D.; Zhou, Y.; Luo, S.; Waluyo, I.; Crumlin, E. J.; Stacchiola, D. J.; Zhou, J.; Carrasco, J.; Busnengo, H. F.; Ganduglia-Pirovano, M. V.; Senanayake, S. D.; Rodriguez, J. A., Dry Reforming of Methane on a Highly-Active Ni-CeO2 Catalyst: Effects of Metal-Support Interactions on C-H Bond Breaking. *Angew Chem Int Ed Engl* **2016,** *55* (26), 7455-9.
23. Akri, M.; Zhao, S.; Li, X.; Zang, K.; Lee, A. F.; Isaacs, M. A.; Xi, W.; Gangarajula, Y.; Luo, J.; Ren, Y.; Cui, Y.-T.; Li, L.; Su, Y.; Pan, X.; Wen, W.; Pan, Y.; Wilson, K.; Li, L.; Qiao, B.; Ishii, H.; Liao, Y.-F.; Wang, A.; Wang, X.; Zhang, T., Atomically dispersed nickel as coke-resistant active sites for methane dry reforming. *Nat. Commun.* **2019,** *10* (1), 5181.
24. Bruix, A.; Rodriguez, J. A.; Ramírez, P. J.; Senanayake, S. D.; Evans, J.; Park, J. B.; Stacchiola, D.; Liu, P.; Hrbek, J.; Illas, F., A New Type of Strong Metal–Support Interaction and the Production of H2 through the Transformation of Water on Pt/CeO2(111) and Pt/CeOx/TiO2(110) Catalysts. *J. Am. Chem. Soc.* **2012,** *134* (21), 8968-8974.
25. Daelman, N.; Capdevila-Cortada, M.; López, N., Dynamic charge and oxidation state of Pt/CeO2 single-atom catalysts. *Nat. Mater.* **2019,** *18* (11), 1215-1221.
26. Brummel, O.; Waidhas, F.; Faisal, F.; Fiala, R.; Vorokhta, M.; Khalakhan, I.; Dubau, M.; Figueroba, A.; Kovács, G.; Aleksandrov, H. A.; Vayssilov, G. N.; Kozlov, S. M.; Neyman, K. M.; Matolín, V.; Libuda, J., Stabilization of Small Platinum Nanoparticles on Pt–CeO2 Thin Film Electrocatalysts During Methanol Oxidation. *J. Phys. Chem. C* **2016,** *120* (35), 19723-19736.
27. Dvořák, F.; Farnesi Camellone, M.; Tovt, A.; Tran, N.-D.; Negreiros, F. R.; Vorokhta, M.; Skála, T.; Matolínová, I.; Myslivečeк, J.; Matolín, V.; Fabris, S., Creating single-atom Pt-ceria catalysts by surface step decoration. *Nat. Commun.* **2016,** *7* (1), 10801.
28. Pereira-Hernandez, X. I.; DeLaRiva, A.; Muravev, V.; Kunwar, D.; Xiong, H.; Sudduth, B.; Engelhard, M.; Kovarik, L.; Hensen, E. J. M.; Wang, Y.; Datye, A. K., Tuning Pt-CeO2 interactions by high-temperature vapor-phase synthesis for improved reducibility of lattice oxygen. *Nat Commun* **2019,** *10* (1), 1358.
29. Bruix, A.; Neyman, K. M.; Illas, F., Adsorption, Oxidation State, and Diffusion of Pt Atoms on the CeO2(111) Surface. *J. Phys. Chem. C* **2010,** *114* (33), 14202-14207.
30. Wang, X.; Yuan, Q.; Li, J.; Ding, F., The transition metal surface dependent methane decomposition in graphene chemical vapor deposition growth. *Nanoscale* **2017,** *9* (32), 11584-11589.
31. Qi, Q.; Wang, X.; Chen, L.; Li, B., Methane dissociation on Pt(111), Ir(111) and PtIr(111) surface: A density functional theory study. *Applied Surface Science* **2013,** *284*, 784-791.

32. Prats, H.; Gutierrez, R. A.; Pinero, J. J.; Vines, F.; Bromley, S. T.; Ramirez, P. J.; Rodriguez, J. A.; Illas, F., Room Temperature Methane Capture and Activation by Ni Clusters Supported on TiC(001): Effects of Metal-Carbide Interactions on the Cleavage of the C-H Bond. *J Am Chem Soc* **2019,** *141* (13), 5303-5313.
33. Martin, N. M.; Van den Bossche, M.; Hellman, A.; Grönbeck, H.; Hakanoglu, C.; Gustafson, J.; Blomberg, S.; Johansson, N.; Liu, Z.; Axnanda, S.; Weaver, J. F.; Lundgren, E., Intrinsic Ligand Effect Governing the Catalytic Activity of Pd Oxide Thin Films. *ACS Catalysis* **2014,** *4* (10), 3330-3334.